Clays and Clay Minerals, Vol. 46, No. 4, 429–435, 1998.

EFFECTS OF SECONDARY IRON PHASES ON KAOLINITE ^{27}Al MAS NMR SPECTRA

PAUL A. SCHROEDER,[1] ROBERT J. PRUETT[2] AND VERNON J. HURST[1]

[1] University of Georgia, Department of Geology, Athens, Georgia 30602-2501

[2] ECC International, Inc., P.O. Box 471, Sandersville, Georgia 31082

Abstract—Eight kaolinite and 2 halloysite samples were analyzed using ^{27}Al magic angle spinning nuclear magnetic resonance (MAS NMR) spectroscopy, chemical analysis and magnetic susceptibility to understand the effect of isomorphously substituted Fe^{3+} and secondary Fe phases on the NMR signal. Known additions of goethite and hematite were made to determine the response of kaolinite ^{27}Al MAS NMR spectra and sample magnetic susceptibilities.

Results from high field (11.7 T) NMR studies show positive correlations between 1) Fe content, 2) magnetic susceptibility and 3) relative intensity of the spinning side band (SSB) to central band (CB) ratio. No correlation is observed between the mass-corrected NMR spectral intensity and Fe content. Comparative high/low field (11.7 T/8.46 T) NMR studies show a decrease in the relative ratio of line broadening with increasing Fe content. Projected trends of known additions of hematite and goethite versus magnetic susceptibility extrapolate back to zero y intercepts that have Fe concentrations higher than actually measured.

Absolute intensity observations have negative implications for the use of ^{27}Al MAS NMR spectroscopy in assessing Fe-ordering in kaolinites. First, high-energy, short ($\frac{1}{6}$ of $\frac{\pi}{2}$ solutions) pulse sequences do not produce reliable quantitative data needed to assess paramagnetic line-broadening affects caused by different Fe-ordering clustering scenarios. The lack of perfect correlation between SSB/CB, Fe content and magnetic susceptibility indicates that differences exist with respect to 1) the amount of isomorphously substituted Fe, 2) the ordering of the Fe within kaolinite, 3) the concentration of secondary Fe phases and 4) magnetic susceptibility of the secondary Fe assemblage. Variability of line-width ratios at different field strengths indicates an increasing second-order quadrupole effect (SOQE) with increasing Fe. Finally, the difference between the observed Fe content and that predicted from magnetic susceptibility measurements suggest that magnetic domain properties of secondary Fe phases behave differently from Fe domains bound in kaolinite.

Key Words—^{27}Al NMR Spectroscopy, Goethite, Halloysite, Hematite, Iron, Kaolinite, Magnetic Susceptibility.

INTRODUCTION

The intimate coexistence of kaolinite, hematite and goethite in many soils and kaolin deposits has made study of their individual crystal-chemical properties difficult. Mineral study is further complicated by the fact that Fe isomorphously substitutes for Al in kaolinite and Al isomorphously substitutes for Fe in goethite and hematite. One approach that has been used to elucidate the nature of Fe-ordering within different kaolinites has been ^{27}Al MAS NMR spectroscopy (Schroeder and Pruett 1996). In their study, attempts were made to chemically remove secondary Fe phases from the kaolinite samples using acid extraction. Although the states of the clays were examined with transmission electron microscopy (TEM) before and after the treatment, the effects of secondary Fe phases on the ^{27}Al NMR signal were still not well understood.

The purpose of this study is to examine the effects of known additions of goethite and hematite on the ^{27}Al NMR spectra of kaolins with different Fe contents. In particular, the spectral properties of 8 kaolinites and 2 halloysites were examined to see the known addition effects on: 1) ^{27}Al NMR spectral intensity, 2) the relative intensities of the SSBs and 3) peak line broadening. Chemical and bulk mass magnetic susceptibility properties were also examined.

MATERIALS AND METHODS

Samples

The kaolinites used in this study were collected from: 1) a geode from Warsaw, Illinois (WR); 2) kaolin hosted by Cretaceous sedimentary rocks, Georgia (KG); 3) kaolin hosted by Eocene sedimentary rocks in Georgia (TG); 4) A kaolinitic clay from Pugu Hills, Dar-es-Salaam, Tanganyika, Tanzania, Africa (PH), (Yale Peabody Museum #MIN 02.6934); 5) a tropical clay from South America (TC); 6) a kaolin from a lateritic weathering profile at Rio Capim, Brazil (RC), described by Hurst and Bósio (1975); 7) a kaolin deposit near the Skardon River, Australia (SR); 8) kaolin hosted by Cretaceous sedimentary rocks from the Chambers #4 mine, Georgia (KC). Two halloysite samples were used in this study, one containing a spherical form (HS) and the other an elongate form (HE). They were collected from a tonstein (HS) and granodiorite (HE) saprolite in Latah County, Idaho, and described by Pruett and Murray (1993).

Table 1. Weight percent oxide and loss-on-ignition (LOI) data and normalized structural formulae for kaolinite and halloysite samples.†

Oxide	KCu	KCt	RCu	RCt	SRu	SRt	SHu	EHu
SiO_2	44.3	44.4	44.3	45.5	44.4	45.8	45.5	46.3
Al_2O_3	37.7	37.7	37.7	38.0	38.7	37.4	37.6	38.0
TiO_2	2.45	2.59	2.23	2.19	1.44	1.54	1.04	0.02
Fe_2O_3‡	0.47	0.34	0.80	0.67	1.33	1.30	0.08	0.32
MgO	0.02	0.02	0.02	0.02	0.06	0.06	0.03	0.03
CaO	0.02	0.02	0.15	0.15	0.07	0.03	0.25	0.03
Na_2O	0.21	0.05	0.09	0.04	0.29	0.08	0.05	0.02
K_2O	0.08	0.08	0.02	0.03	0.09	0.08	0.05	0.01
LOI§	13.9	14.0	13.9	13.9	14.1	14.1	15.1	15.4
				Tetrahedral				
Si	—	1.99	—	2.00	—	2.01	2.02	2.03
Al	—	0.01	—	0.00	—	0.00	0.00	0.00
Total		2.00		2.00		2.01	2.02	2.03
				Octahedral				
Al	—	1.99	—	1.97	—	1.94	1.97	1.96
Fe(III)	—	0.01	—	0.02	—	0.04	0.00	0.01
Total		2.00		1.99		1.98	1.97	1.97
OH	—	4.00	—	4.00	—	4.00	4.00	4.00
Excess H_2O	—	0.10	—	0.04	—	0.07	0.20	0.25

† See text for sample ID descriptions. u = untreated, t = treated with HCl.
‡ Fe oxide is total Fe(II) + Fe(III).
§ LOI is calculated at molar H_2O. Excess OH sites recast as molecular H_2O with the number of tetrahedral sites set at 2 and OH sites set at 4, assuming 7 O equivalents per unit formula.

Known quantities of the minerals hematite and goethite were added to selected kaolinite samples at levels of 1 to 2% by weight. The hematite (from Graves Mountain, Georgia) was ground into a powder before weighing and mixing. The goethite sample was obtained from a lateritic weathering profile in Brazil. Each was checked for purity using X-ray powder diffraction (XRD). Additional XRD analysis using the method of Schulze (1984) indicated the goethite has approximately 10% Al-for-Fe substitution in the structure.

Analytical Methods

The HCl acid treatment used for extraction of secondary Fe is detailed in Schroeder and Pruett (1996). Extractable Fe and Al contents were measured using the solution extract. Fe was measured using atomic absorption spectroscopy (AAS) and Al with a Perkin-Elmer induction-coupled plasma mass spectrometer (ICP-MS), both at the University of Georgia's Department of Crop and Soil Science. Soluble Al was measured on the extract to detect for potential contemporaneous aluminosilicate dissolution (this was not done in the previous study by Schroeder and Pruett 1996).

Major oxide analyses of both the treated and untreated samples were conducted using a Perkin-Elmer Plasma 40 ICP-atomic emission spectrometer calibrated using known kaolinite reference materials. Samples were prepared by fusing with $LiBO_2$ at 1050 °C in a graphite crucible. The resulting glass was dissolved in 3% HNO_3 and 1% HF. Loss on ignition (LOI) was determined gravimetrically by heating the sample in a muffle furnace to 1050 °C for 1 h.

Magnetic susceptibility measurements were made using a Johnson-Matthey® magnetic susceptibility balance. The balance replaces the traditional Gouy balance system and makes a direct mass susceptibility measurement after calibration with a known reference material ($HgCO(SCN)_4$). The mass susceptibility (χ_g) is defined as the ratio of intensity of the magnetism induced in a substance to the intensity of the applied field divided by the material density. Units are given in cm^3/g.

The ^{27}Al MAS-NMR studies were conducted using an 11.74-T magnet (^{27}Al Larmor frequency = 130.24 MHz, ^1H Larmor frequency = 360 MHz) housed at the University of Illinois at Urbana. The spectrometer was equipped with a Doty Scientific 5-mm high-speed spinning probe and Nicolet 1280 data system. Spectra were collected at spinning speeds of 11 kHz, using a 4-phase cycle pulse (CYCLOP) sequence. The CYCLOP spectra, used for quantitation, were collected with a pulse length of 1.0 μs (⅙ of a solution ½ pulse), recycle delay of 2 s and 200 acquisitions. Peak intensities were determined by an integrating routine and then normalized by the sample mass (ca. 100 mg) packed into a Si_3N_4 rotor.

RESULTS

Table 1 shows chemical oxide analyses for the kaolinites and the halloysites for which data have not been previously published (Schroeder and Pruett

https://doi.org/10.1346/CCMN.1998.0460407 Published online by Cambridge University Press

Table 2. Sample identifications, ^{27}Al NMR intensity, FWHM, SSB to CB ratio, χ_g and Fe content.

Sample ID†	Sample description (relative wt% added)	^{27}Al intensity per mg sample	FWHM (ppm)	SSB/CB ratio	χ_g 10^{-6} cm^3/g	%Fe by weight‡
HEu	Elongate halloysite, saprolite, Idaho, untreated	8.79	7.8	0.054	1.60	0.22
HSu	Spherical halloysite, tonstein, Idaho, untreated	7.24	8.1	0.060	−0.02	0.06
KCu	Chambers #4, Ga., Cretaceous-hosted, untreated	7.35	7.8	0.054	0.32	0.33
KCt	Chambers #4, Ga., Cretaceous-hosted, HCl-treated	8.62	8.0	0.068	0.16	0.24
KGu	Cretaceous-hosted, Georgia, untreated	8.97	7.9	0.071	0.12	0.27
KGt	Cretaceous-hosted, Georgia, HCl-treated	8.02	7.8	0.059	0.08	0.23
KGtg1	Cretaceous-hosted, Georgia, HCl-treated, goethite (0.74)	8.65	7.7	0.057	0.42	0.68
KGtg2	Cretaceous-hosted, Georgia, HCl-treated, goethite (2.41)	8.33	7.8	0.054	1.24	1.69
PHu	Pugu Hills, Africa, untreated	5.99	8.7	0.105	1.40	0.92
PHt	Pugu Hills, Africa, HCl-treated	7.03	8.7	0.093	1.30	0.90
PHug1	Pugu Hills, Africa, untreated, goethite (0.77)	6.63	8.6	0.105	2.84	1.34
PHuh1	Pugu Hills, Africa, untreated, hematite (1.09)	8.86	8.5	0.105	2.50	1.68
PHuh2	Pugu Hills, Africa, untreated, hematite (2.69)	6.75	8.7	0.116	3.42	2.80
RCu	Cretaceous-hosted, Rio Capim, Brazil, untreated	8.60	7.8	0.068	0.78	0.56
RCt	Cretaceous-hosted, Rio Capim, Brazil, HCl-treated	7.93	7.9	0.066	0.71	0.47
SRu	Skardon River, Australia, untreated	7.45	8.3	0.093	1.34	0.93
SRt	Skardon River, Australia, HCl-treated	6.91	8.3	0.090	1.35	0.91
TCu	Tropical Clay, untreated	6.63	8.3	0.116	2.30	1.27
TCt	Tropical Clay, HCl-treated	7.25	8.0	0.114	2.30	1.24
TCtg1	Tropical Clay, HCl-treated, goethite (1.23)	6.88	8.3	0.120	3.53	2.01
TCtg2	Tropical Clay, HCl-treated, goethite (3.65)	6.75	8.5	0.139	4.44	3.54
TCth1	Tropical Clay, HCl-treated, hematite (0.92)	6.73	8.3	0.133	3.04	1.91
TCth2	Tropical Clay, HCl-treated, hematite (2.27)	7.49	8.5	0.122	4.02	2.83
TGu	Tertiary-hosted, Georgia, untreated	9.13	7.9	0.079	1.20	0.78
TGt	Tertiary-hosted, Georgia, HCl-treated	7.15	8.0	0.082	1.11	0.70
TGtg1	Tertiary-hosted, Georgia, HCl-treated, goethite (0.95)	7.31	8.1	0.085	2.02	1.30
WRu	Warsaw, Illinois, Geode, untreated	8.12	7.4	0.068	0.45	0.08
WRt	Warsaw, Illinois, Geode, HCl-treated	7.60	7.4	0.041	−0.05	0.02
WRth1	Warsaw, Illinois, Geode, HCl-treated, hematite (1.35)	8.19	7.4	0.051	0.98	0.97
WRth2	Warsaw, Illinois, Geode, HCl-treated, hematite (2.18)	8.59	7.4	0.054	1.59	1.56

† u = untreated, t = HCl treated.

‡ Samples containing goethite have been recast to account for Al and H_2O content and stochiometric differences.

1996). Also included are oxide analyses for the HCl-extracted samples. As stated earlier, the solutions were analyzed to detect for potential contemporaneous aluminosilicate dissolution. The average solid Al content is about 100 times greater than the Fe content (Table 1). We report here that the soluble Al concentrations of the extracts are on the order of 50 ppm, while the soluble Fe concentrations ranged from 4 to 15 ppm. The proportion of Al released into solution is therefore 10 times less than that for the amount of Fe in the solid. Considering that a small proportion of the soluble Al is derived from hematite and goethite dissolution, the extractable Fe and Al values support the notion that minimal aluminosilicate dissolution occurs during the described HCl treatment.

^{27}Al NMR Integrated Intensities

Table 2 presents the experimental results of ^{27}Al NMR intensity, SSB/CB, full width at half maximum (FWHM) as well as Fe content and χ_g measurements. All other intrinsic sample and instrumental factors being equal, theory predicts that the relative amount of Al "seen" in an ^{27}Al NMR experiment should be related to amount and ordering of Fe substituted in the crystal lattice (Schroeder 1993). The most immediate observation made from these data is that there is very little correlation between ^{27}Al NMR spectral intensity and the properties of either Fe content or χ_g.

The lack of correlation between absolute intensity and the quantity of paramagnetic Fe centers indicates that accuracy and precision of intensity measurements are compromised by instrumental conditions (that is, choice of pulse program) and/or that there are variable spatial relations of Fe centers in the kaolinites (that is, short- to long-range ordering or clustering of Fe). Repeated intensity measurements of the same sample (WRt) yielded a precision range of ±0.4 intensity units per mg of sample. This range of reproducibility in the ^{27}Al NMR absolute intensity is too wide to utilize the data for quantitative analysis of paramagnetic line broadening effect and signal wipeout due to Fe centers. These results also bring into question the specific use of the "hard" pulse CYCLOP programming sequence for absolute quantitation.

The use of short, hard pulse sequences at high fields for semiquantitative analysis has seen great success in many clay studies (such as Kinsey et al. 1985; Kirkpatrick and Weiss 1987; Schroeder 1993). For relative

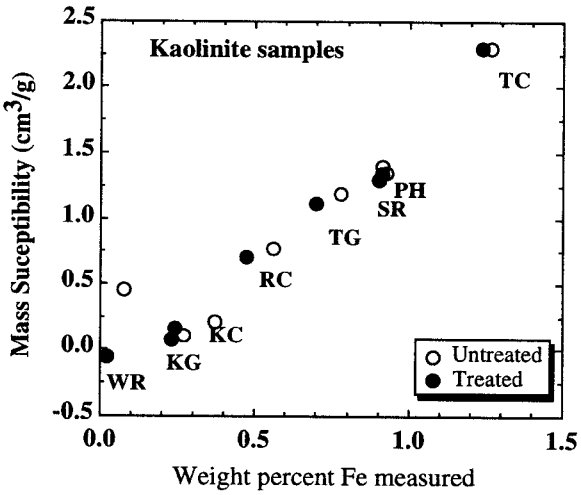

Figure 1. Weight percent Fe measured in natural and HCl-treated samples plotted versus mass susceptibility for the kaolinite specimens. Open circles represent values for untreated samples and solid circles are values for HCl-extracted samples.

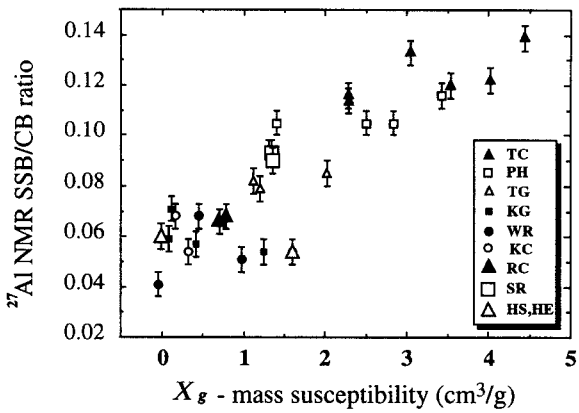

Figure 2. Mass susceptibility plotted versus the ratio of ^{27}Al MAS NMR SS band peak heights to the CB peak height. Vertical bars represent the precision range based on repeated experiments of 1 sample.

estimates of tetrahedral versus octahedral Al, such pulse sequences appear to work well. In the case of this study, it is apparent that absolute quantitation has been compromised by 2 factors related to pulse sequence. As noted by Massiot et al. (1990), the presence of satellite transitions (non-½ integer contributions) to the central transition in the side bands can significantly affect quantitation. Our spectra show that satellite transitions were contributing to the intensity in the spinning side bands.

A second pitfall that results from using short, high-energy pulses is the effect of pulse breakthrough. This is a consequence of high energy that is applied during the CYCLOPS sequence. It is essential to be able to record the free induction decay (FID) with smallest possible delay after the rf pulse. Fukushima and Roeder (1981) have noted, however, that amongst the various difficulties, there may be a need for significant deadtime after the pulse because of ringing and instrument saturation. If the deadtime is too short, then the manifestation of pulse breakthrough can be seen. One solution is to phase-shift the signal before Fourier-transforming the data into the frequency domain. Although the FID were not phase-shifted in this study, it is likely that deadtime was too short.

More recently, Haase and Oldfield (1996) have shown successful quantitative results of noninteger spin quadrupolar nuclides in static solids. Haase and Oldfield (1996) use a 2-pulse spin-echo sequence, where the central transition is selectively excited. Since these "soft pulse" methods were not used in our study, their likelihood for success could not be evaluated. Such investigations may lead to more accurate and precise Al quantitation.

DISCUSSION

^{27}Al Spectral, Fe Content and χ_g Properties

Figure 1 shows the close correlation between the Fe content of untreated and treated kaolinite samples and their χ_g. Each kaolinite exhibits slightly smaller values for both Fe and χ_g after extraction. These results support the notion that the HCl treatment removes some of the secondary antiferromagnetic and/or paramagnetic phases.

The spiking method, using antiferromagnetic materials, was employed to see if the χ_g properties of the kaolinites could be attributed to similar antiferromagnetic or paramagnetic domains that may actually be part of the kaolinite structure (that is, regions within the octahedral sheet that contain clusters of Fe centers). The χ_g values used in this study were measured at 55×10^{-6} cm^3/g for the hematite and 56×10^{-6} cm^3/g for the goethite and are similar to published values (Hunt et al. 1995).

The influence of antiferromagnetic and ferromagnetic centers on SSB intensities has been previously documented for several natural aluminosilicates (Oldfield et al. 1983). Figure 2 shows the relationship between the relative intensity of the SSB (that is, SSB/CB ratio) and χ_g for kaolin minerals. Included in this plot are samples for which the antiferromagnetic minerals hematite and goethite were added (Table 2). Since χ_g originates primarily from the presence of paramagnetic Fe centers, the expected correlation between Fe content and SSB/CB is seen (Figure 3).

Although there is a generally positive correlation between Fe content and relative SSB intensity for all samples, the effect of known Fe additions is variable on an individual sample basis. For example, the geode kaolinite (WR) and the Georgia kaolinite (TG) show a slightly negative correlation with the relative SSB intensity, decreasing with added Fe content. This lack

https://doi.org/10.1346/CCMN.1998.0460407 Published online by Cambridge University Press

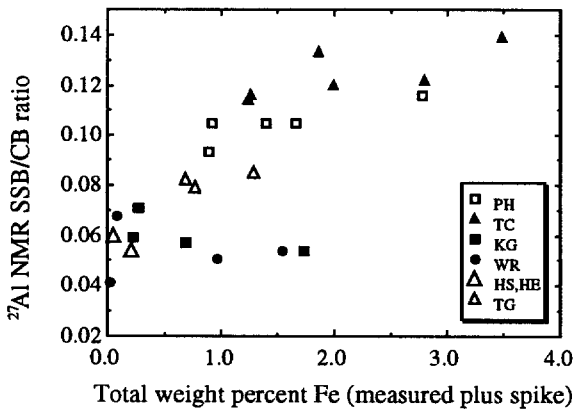

Figure 3. Weight percent Fe (including samples with known Fe additions) plotted versus the ratio of ^{27}Al MAS NMR SS band peak height to the CB peak height.

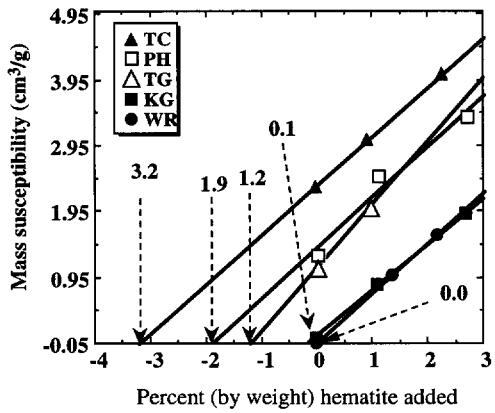

Figure 4. Weight percent of known additions of hematite to 5 kaolinites plotted versus mass susceptibility. Solid lines represent a linear least-squared fit to the data points. Arrows point to the y zero intercept with their respective x intercept value.

of consistent intrasample correlation indicates that the intrinsic Fe remaining in the kaolinite structure behaves variably in the presence of antiferromagnetic phases. The sometimes, positively-, zero- and negatively sloped correlations from sample to sample shows that Fe in the different kaolinite lattices is affecting the SSB in different ways.

Figure 4 shows a plot of percent hematite added to 5 of the kaolinite samples versus the measured χ_g. A linear regression for each data set is included on the plot. The virtually Fe-free geode kaolinite (WR) shows a zero abscissa (y) intercept at the point of diamagnetism (that is, the point at which $\chi_g < 0$). Projection of each sample's linear fit back to the zero y intercept provides an indication of the unknown amount of Fe present if it was responding with the same χ_g properties as hematite. In other words, this analysis assumes that the intrinsic Fe content contributes the same χ_g effect as hematite. That this assumption is incorrect can be shown by comparing the independently measured Fe content to that predicted from the spiking and χ_g measurements.

Figure 5 reveals that the spiking method overestimates the Fe content for samples containing more than 1% Fe_2O_3 content, an indication that the magnetic domains in the Fe-rich kaolinites have a significantly lower χ_g response than the equivalent amount of pure hematite added to each sample. However, the effective χ_g contribution by paramagnetic Fe centers is not linear from sample to sample. The farther above the 1:1 prediction in Figure 5, the less effective the χ_g contribution. This can be explained by the degree of Fe clustering in the kaolinite structure. The tropical clay (TC), although having the highest Fe content, would have a lower predicted χ_g value for its given Fe content (using the relationship in Figure 5). This can be explained with the idea that the Fe centers in the lattice of the tropical clay are less clustered than, for example, in the Georgia kaolinite (TG).

One mitigating factor in the above interpretation is the nature of the hematite crystal domain sizes. It has long been recognized that the magnetostatic self-energy of a crystal is reduced by a greater amount as the surface polarization is broken into a small number of domains (O'Reilly 1984). As the Fe domains get smaller, their effect on χ_g becomes less.

The hematite and goethite domains in this study were not directly measured using high-resolution transmission electron microscopy (HRTEM); however, they could be qualitatively assessed from the XRD peak widths (not shown). XRD patterns indicate that the dimensions of the coherent scattering domains for the hematite added as spiking material likely exceed the dimensions of hematite found naturally in kaolinites. This points out the fact that the effect of second-

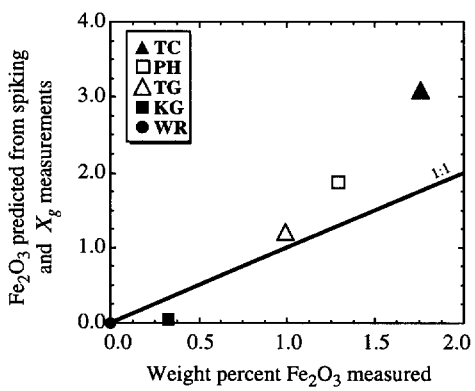

Figure 5. Predicted Fe_2O_3 content of kaolinites based upon hematite spiking method and mass susceptibility measurements plotted versus measured Fe_2O_3 content. The line is a 1:1 reference slope.

https://doi.org/10.1346/CCMN.1998.0460407 Published online by Cambridge University Press

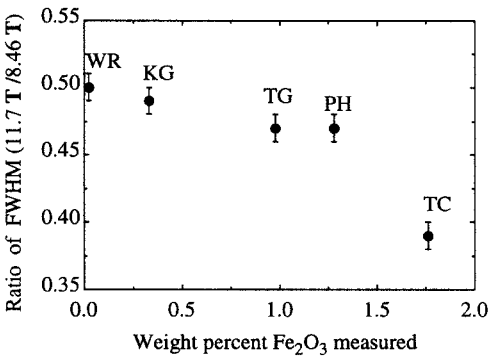

Figure 6. Ratio of FWHM measured in ppm at 11.7 T and 8.46 T plotted versus the weight percent Fe_2O_3. Vertical error bars denote the range of values observed after repeated measurements of the geode kaolinite (WR).

ary Fe-phases on bulk magnetic and NMR spectral properties may be better evaluated if the domain sizes of spiking material accurately duplicate the domains found in natural samples.

NMR Line Broadening Effects

Line broadening (LB) effects, as manifested in the measurement of FWHM, were obtained for each spectra (Table 2). Generally positive correlations exist between the FWHM and the properties of relative SSB intensity, χ_g and Fe content. This result strongly suggests the presence of paramagnetic LB as 1 component of several LB mechanisms contributing to the NMR spectra.

One LB mechanism that is not totally alleviated by MAS is the SOQE (Kirkpatrick 1988). As discussed by Schroeder (1993), the relative magnitude of the SOQE can be assessed by examining the same set of samples at 2 different field strengths. Five samples used in this study were previously investigated by Schroeder and Pruett (1996) at 8.46 T. The FWHM were measured, in ppm, at 14.7 for WRt, 16.0 for KGt, 16.9 for TGt, 18.5 for PHt and 20.6 for TCt.

Figure 6 shows a plot of the ratio of line widths (in ppm) at field strengths 11.7 T and 8.46 T versus Fe content. The ratios range from about 0.5 for WR to 0.37 for the TC, thus indicating an increase in the amount of SOQE with increase in Fe content. Included in the SOQE is an asymmetry parameter that reflects a nonspherical distribution of charge around the nucleus. An increase in SOQE reflects the fact that there are larger nonzero electric field gradients surrounding Al sites. This relative increase in the asymmetry of the charge distribution around the Al sites within the TC indicates that sites are more distorted from an ideal octahedral coordination when compared to the Al sites in the other 4 kaolinites. The WR exhibits the smallest ratio, thus indicating a structure containing Al with the least amount of octahedral site distortion. The simple addition of Fe, either as hematite or goethite, does not significantly affect the FWHM (see data in Table 2), and it is likely that relative ratios of the FWHM in the spiked samples would reflect the same trend of increasing SOQE with increasing isomorphous Fe.

The untreated elongate form of halloysite (HEu) in this study contains more Fe and has a higher χ_g and has less NMR LB when compared to the spherical form (HSu). This negative correlation between Fe content and LB contrasts the observation and conclusions of Newman et al. (1994). They suggest paramagnetic dipole-dipole interactions between structural Fe and Al as the main cause for line broadening in halloysites. The spherical form is virtually Fe-free, which would indicate that almost all LB comes from the SOQE. Although multifield strength measurements were not made on the halloysites, the similarity between the line widths of the Fe-free geode kaolinite and the spherical form (Table 2) indicate SOQE as the principal line broadening mechanism in the spherical halloysite.

CONCLUSIONS

The relative decreases in χ_g and SSB intensity that result from acid extraction are consistent with idea that Fe extracted from kaolinites is derived from material with χ_g values similar to (but not the same as) hematite and goethite. The effect of known additions of hematite and goethite (antiferromagnetics) on kaolinite ^{27}Al NMR spectra is to generally produce a small increase in χ_g and SSB intensity. This is attributed, in part, to the larger magnetic domain sizes of spiking material relative to magnetic domains in kaolinite. On an individual sample basis, the relative SSB intensities do not correlate with the total Fe content or χ_g resulting from known additions. This suggests that Fe ordering schemes are variable amongst different kaolinites and the amount of Fe will have variable influence on kaolinite χ_g and SSB behavior.

Short ($\frac{1}{6}$ of $\frac{\pi}{2}$ solutions) pulse sequences do not produce reliable absolute intensity data needed to assess paramagnetic line-broadening affects caused by different Fe ordering-clustering scenarios. Variability of line-width ratios measured for 5 kaolinites at different field strengths indicate an increasing SOQE with increasing Fe. Future efforts should include a study of the effects of secondary Fe-phase magnetic domain sizes and spin-echo pulse sequences for more accurate quantitative Al measurements.

ACKNOWLEDGMENTS

Thanks are extended to ECC International for approval to publish the results and financial support of the NMR spectroscopy. This work benefited from the insights of B. Montez and J. Kirkpatrick. The authors, however, are solely responsible for interpretations. W. Andrews was helpful for performing chemical analysis and sample preparation. This project was partially supported by the University of Georgia Research Foundation, Inc., and acknowledgment is made to the

donors of the Petroleum Research Fund, administered by the American Chemical Society, for support of this research (ACS-PRF #29072-G2 to the senior author).

REFERENCES

Fukushima E, Roeder SBW. 1981. Experimental pulse NMR: A nuts and bolts approach. Reading, MA: Addison-Wesley Publ. 539 p.

Haase J, Oldfield E. 1996. Quantitative determination of non-integer spin quadrulpole nuclei in solids using nuclear magnetic spin-echo techniques. J Mag Res 104:1–9.

Hunt CP, Moskowitz BM, Banerjee SK. 1995. Magnetic properties of rocks and minerals. In: Ahrens TJ, editor. Rock physics and phase relations: A handbook of physical constants. Washington, DC: Am Geophysical Union. p 189–204.

Hurst VJ, Bósio NJ. 1975. Rio Capim kaolin deposits, Brazil. Econ Geol 70:990–992.

Kinsey RA, Kirkpatrick RJ, Hower J, Smith KA, Oldfield E. 1985. High resolution aluminum-27 and silicon-29 nuclear magnetic resonance spectroscopic study of layer silicates, including clay minerals. Am Mineral 70:537–548.

Kirkpatrick RJ. 1988. MAS NMR spectroscopy of minerals and glasses. In: Hawthorne FC, editor. Spectroscopic methods in mineralogy and geology. Rev Mineral. Washington, DC: Mineral Soc Am. p 341–404.

Kirkpatrick RJ, Weiss CA. 1987. Magic-angle sample-spinning NMR spectroscopy of clay minerals. In: Stucki JW, Banwart WL, editors. NATO conference volume on analytical chemical methods in clay minerals research. Boston, MA: D. Reidel Publ. 465 p.

Massiot D, Bessada C, Courures JP, Taulelle F. 1990. A quantitative study of ^{27}Al MAS NMR in YAG. J Mag Res 90: 231–242.

Newman RH, Childs CW, Churchman GJ. 1994. Aluminum coordination and structural disorder in halloysite and kaolinite by ^{27}Al NMR spectroscopy. Clay Miner 29:305–312.

Oldfield E, Kinsey RA, Smith KA, Nichols JA, Kirkpatrick RJ. 1983. High-resolution NMR of inorganic solids. Influence of magnetic centers on magic-angle sample-spinning lineshapes in some natural aluminosilicates. J Mag Res 51: 325–329.

O'Reilly W. 1984. Rock and mineral magnetism. New York: Blackie. 220 p.

Pruett RJ, Murray HH. 1993. The mineralogical and geochemical controls that source rocks impose on sedimentary kaolins. In: Murray H, Bundy W, Harvey C, editors. Kaolin genesis and utilization. Boulder, CO: Clay Miner Soc. p 149–170.

Schroeder PA. 1993. A chemical, XRD and ^{27}Al NMR investigation of Miocene Gulf Coast shales with application to understanding illite/smectite crystal-chemistry. Clays Clay Miner 41:668–679.

Schroeder PA, Pruett RJ. 1996. Iron ordering in kaolinites: Insights from ^{29}Si and ^{27}Al NMR spectroscopy. Am Mineral 81:26–38.

Schulze DG. 1984. The influence of aluminum on iron oxides. VIII. Unit-cell dimension of Al-substituted goethites and estimation of Al from them. Clays Clay Miner 32:36–44.

(Received 31 January 1997; accepted 5 November 1997; Ms. 97-011)